Pol. J. Environ. Stud. Vol. 24, No. 1 (2015), 375-380

Original Research

Organic Matter and Nitrogen Distribution, and Functional Groups of Filter at Earthworm Packing Bed in Vermifiltration

Fei Yang[1], Longmian Wang[2], Guoxiang Wang[1], Peng Du[3], Yimin Zhang[2]*

[1]School of Geography Science, Nanjing Normal University, Nanjing 210023, P. R. China
[2]Nanjing Institute of Environmental Sciences, Ministry of Environmental Protection, Nanjing 210042, P. R. China
[3]Sino-Japan Friendship Center for Environmental Protection, Ministry of Environmental Protection, Beijing 100029, P. R. China

Received: 20 July 2014
Accepted: 5 September 2014

Abstract

This paper studies organic matter (OM) and nitrogen (N) distributions at different depths of an earthworm packing bed, and the N distribution *in situ* solution in artificial soil (AS). The contents of OM, nitrate nitrogen (NO_3-N), ammonia nitrogen (NH_3-N), and total nitrogen (TN) changed along with the depth of AS. The results of N concentration *in situ* solution indicated that 35 cm to 40 cm thickness of earthworm packing bed thickness was optimal for removing NH_3-N and TN for synthetic wastewater treatment. Fourier transform infrared spectra showed that most intensity variations of the absorbance peaks increased in AS, decreased in detritus, and slightly changed in sand after synthetic wastewater treatment. Furthermore, certain functional chemical attributes might evaluate the OM contents at the VF media, and AS could act as the main matrices for OM reaction.

Keywords: earthworm, FTIR spectra, nitrogen, organic matter, vermifilter

Introduction

Non-point source pollution, especially rural domestic sewage, has a negative impact on the natural environment and human life. Thus attention has been given to wastewater processing technologies of high efficiency and low consumption to promote water conservation and water pollution control. Many technologies have been applied for the removal of contaminants from rural domestic sewage. Examples include the use of constructed wetland systems planted with Typha orientalis and Phragmites to treat rural domestic wastewater in autumn [1]; a novel multistep bio-ecological system consisting of a biological unit and an ecological post-treatment unit for rural wastewater treatment [2]; and a moving-bed sequencing batch reactor system with held medium to dispose of sewage [3]. These processes have their own advantages and are effective for wastewater treatment in rural areas. According to the characteristics of rural sewage, the treatment technologies must be cost-effective and easy to adopt; they must also require less energy input and maintenance costs, and be capable of meeting effluent discharge standards. Therefore, the desired method is one that performs well, has lower construction and operational costs, and is easy to manage and maintain.

Vermifiltration (VF), a wastewater treatment technology, is designed based on earthworm ecological functions to improve soil permeability and promote organic matter decomposition [4]. It is an environment-friendly and economically feasible technology for domestic sewage treatment in rural areas [5]. Previous studies focused on its

*e-mail: zym@nies.org

application to remove suspended solids (SS), chemical oxygen demand (COD), nitrogen (N), and phosphorus (P) of domestic wastewater efficiently; and used an integrated technology including VF for better nutrient removal [4, 6]. Aside from its application in domestic wastewater, VF's mechanism for N and P removal in synthetic domestic wastewater treatment has also been studied [7, 8]. Although sewage treatment by VF and some of its influencing factors and pollutant removal mechanisms have been studied, the organic matter (OM) and N distribution in filter and the changes in the functional groups of the substrates have yet to be determined or evaluated.

The objectives of the current study are as follows:

(1) To compare OM distributions at different depths of matrices
(2) To determine the N distribution of the earthworm packing bed and *in situ* solution
(3) To analyze the Fourier transform infrared (FTIR) spectra of substrates at different substrates before and after sewage treatment for an in-depth knowledge of OM and N distribution in the VF.

Experimental Procedures

Experimental Design

The schematic diagram of the laboratory-scale experimental apparatus is shown in Fig. 1. The VF apparatus is 30 cm × 30 cm in dimension, with 75 cm depth and 70 cm packed padding. Three padding sampling holes 30 mm in diameter are distributed on the lateral surface of the apparatus. Cobblestone (5 cm thickness, 10 mm to 50 mm particle size), detritus (15 cm thickness, 3 mm to 10 mm particle size), silver sand (15 cm thickness, 100 μm to 800 μm particle diameter), and earthworm packing bed (35 cm thickness) were poured into the microbial-earthworm ecofilter, respectively. An earthworm packing bed consisting of artificial soil (AS) (mixed with soil and rice straws, with a volume ratio of 4) and *Eisenia fetida* (Savigny) were used in the experiments. Before all were installed into the apparatus, the rice straws were pretreated using the method by Shao et al. [9]. Synthetic wastewater was pumped into the wastewater distributor, and then made to flow through the VF.

In the experiment, the surface loading of wastewater was adjusted to 0.2 $m^3/m^2 \cdot d$. The influent quality of the laboratory-scale experimental apparatus is shown in Table 1, based on the method by Fang et al. [7]. Each running cycle included 2 h of wastewater flow, 1 h of retention, water emptying, and, finally, 21 h of drying. The device was in motion to determine the OM, N distribution, and FTIR spectra in the media. In addition, the test was conducted for approximately 2 months.

Samples and Data Analysis

The water samples were collected from the influent and *in situ* solution of the AS in VF at the end of the operational period. All samples were stored at 4ºC for less than 24 h before analysis, and three replicates were assessed for every indicator in each sample. According to the Chinese National Standard (CNS) methods (water and wastewater monitoring and analysis methods, 2002) [10], which comply with the standard methods of the American Public Health Association/American Water Works Association/ Water Environment Federation, the COD, ammonia nitrogen (NH_3-N), total nitrogen (TN), and total phosphorus (TP) concentrations were determined via the potassium dichromate method, Nessler's reagent colorimetric method, potassium persulfate oxidation-ultraviolet spectrophotometric method, and molybdenum-antimony anti-

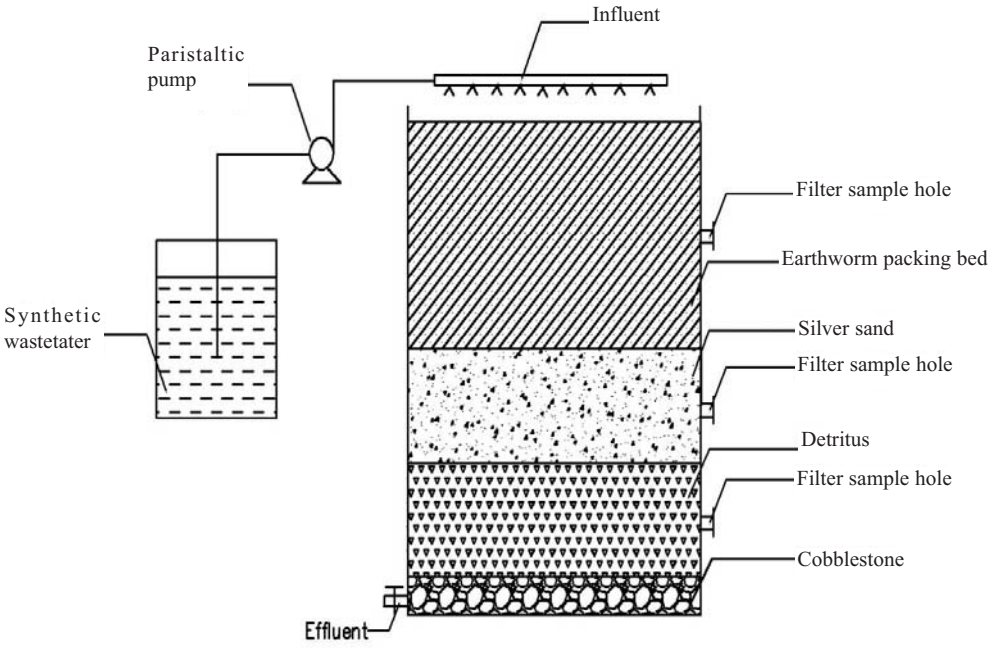

Fig. 1. Schematic diagram of the laboratory-scale experimental apparatus.

Table 1. Water quality of the synthetic domestic sewage at the influent.

Water quality index	pH	Temperature (ºC)	DO (mg/L)	COD (mg/L)	TN (mg/L)	NH_3-N (mg/L)	TP (mg/L)
Values*	7.68±0.32	28.65±1.56	4.67±0.48	256.78±10.86	51.82±5.31	46.27±7.69	3.16±0.25

*Values (mean±standard deviation) are averages of three replicates.

Table 2. Physicochemical characteristics of initial fillings*.

Items	Unit	Artificial soil	Sand	Detritus
Porosity	%	47.5±2.2	27.6±1.5	19.5±2.8
Bulk density	g/cm^3	1.14±0.06	1.86±0.23	2.03±0.02
Permeability coefficient	cm/s	4.7×10^{-3}±0	0.019±0.002	0.46±0.07
pH		7.04±0.12	8.53±0.23	9.24±0.45
OM	g/kg	76.4±1.4	5.8±0.7	11.2±0.3
TN	g/kg	5.3±0.6	—**	—**
NH_3-N	g/kg	1.5±0.1	—**	—**
NO_3-N	mg/kg	25.2±1.8	—**	—**

*All data represent the average of triplicates (mean±standard deviation).
**Data are negligibly small.

spectrophotometric method, respectively. The spectrophotometric method was used to determine nitrate nitrogen (NO_3-N). Dissolved oxygen (DO) content was measured *in situ* using a portable DO meter (YSI Model no. 550A, USA) when water samples were examined. The pH was detected using a PHS-2C pH meter (Shanghai Kangyi Instrument Co. Ltd., China).

AS, silver sand, and detritus were collected before and after the operational period from padding sample holes at the VF. Meanwhile, final AS at different depths in an earthworm packing bed were collected via intermittent destruction. Subsequently, plant roots, earthworms, and other wastes were removed from the substrates. Table 2 presents several physicochemical characteristics of the initial fillings. All characteristics were air-dried at room temperature and gently ground to pass through an 80-mesh sieve. The porosity and bulk density were measured using standard soil science methods [11]. By applying the penetration tube method to detect the permeability coefficient, the pH value was determined in a 1:5 solid-water mixture using a pH meter. The OM was analyzed as the loss on ignition at 550ºC for 2 h [11]. The functional groups were tested using a Nexus 870 infrared spectrometer (USA). The TN, NH_3-N, and NO_3-N concentrations in the filters were determined via the semi-microkelvin method, 10% of KCl extraction-distillation method, and Cu-Cd reduction-colorimetry method, respectively [11]. Three replicates were assessed for each indicator in each sample.

All statistical analyses, including the control, were conducted using Origin 8.0 software.

Results and Discussion

OM Content Distribution at Different Matrices

The OM contents in the initial AS were shown to be higher than in the sand and detritus (Table 2). Comparing the OM quantities in the three media before and after the operational period, the OM in AS increased obviously (Fig. 2), whereas the changes in the sand and detritus were slight (the following data were not included in the tables or figures: final sand, 6.3 g/kg; final detritus, 7.6 g/kg). The results also showed that the OM concentrations in the AS increased at first, and then decreased along the earthworm packing bed depth, and the peak was from 10 cm to 20 cm.

By comparison, soil is abundant in OM, composed of the roots of plants, remains of small animals, residues of plants and animals, humus, and microorganisms [12]. In addition, Wang et al. [8] reported that soil, the main medium affecting the processes in VF, is more beneficial for the removal of organic contaminants via precipitation and adsorption than silver sand and detritus. Thus most OM from the wastewater entered the soil, resulting in a significant OM increase in soil, but a slight variation occurred in other media. With respect to the change in OM content along the depth gradient of the earthworm packing bed, sewage first passed through the upper soil, and then moved to the subsoil due to gravity. The contact time between the sufficient OM of wastewater and topsoil was too short, and the gradual degradation of OM at the influent resulted in an increase in AS OM content followed by reduction. Meanwhile, the production of OM-rich wormcast through the activity of *E. fetida*, which mainly live within the depths of 10 cm to 25 cm, caused the maximal OM content at middle-level AS.

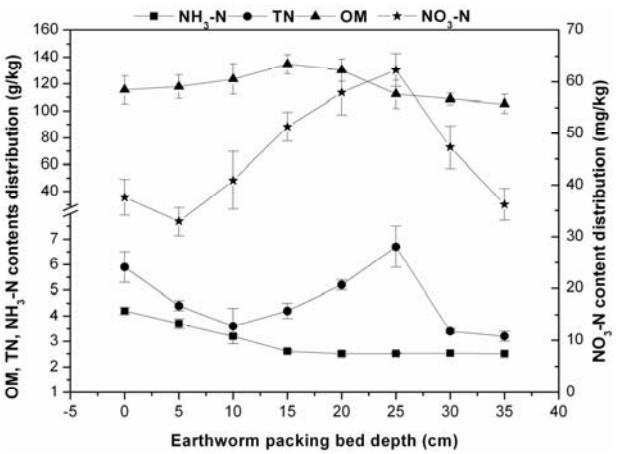

Fig. 2. Organic matter and nitrogen distribution in earthworm packing bed (artificial soil).

N Distribution of the Earthworm Packing Bed and *in situ* Solution

Nitrogen distribution in the final padding of the AS is shown in Fig. 2, which indicates that NH_3-N decreased with increasing sampling depth. Initially when the wastewater was distributed to the ecofilter, the NH_3-N at the influent was adsorbed by soil particles because of electrostatic attraction and the lattice fixation of clay minerals [13]; hence the NH_3-N content in the final AS was higher than that in the initial AS (Table 2). Subsequently, the NH_3-N content dramatically decreased from the surface to the sampling depth of 15 cm, and the NH_3-N content slowly decreased, reaching a relatively low level when the sampling depth exceeded 15 cm. In the superstratum, the high DO concentration from the influent (4.67 mg/L) provided higher degrees of earthworm packing bed oxygenation and consequent removal of AS ammonia via nitrification. The slow decrease may be because NH_3-N reached the adsorbed equilibrium presented in the upper AS, which did not leach along with the water flow, and the decreasing DO along with the depth was not suitable for nitrification.

Compared with TN and NH_3-N, the NO_3-N content was relatively low in all AS, and its content was slightly higher in every final soil than that in the initial soil. Similar to that in constructed wetlands, negatively charged nitrates in sewage is not easily trapped by soil particles, mostly staying with the effluent [14]. The NO_3-N content in the AS increased after treatment because of rice straw introduction, which has NO_3-N adsorption ability, although its anion adsorbtion capacity is limited [15]. Fig. 2 also presents the slight decrease in NO_3-N from 0 cm to 5 cm, and in TN from 0 cm to 10 cm; also shown is an obviously increasing trend from 5 and 10 cm to 25 cm, following a sharp decline of 25 cm for both in the final padding. Clearly, the decrease in TN and NO_3-N in the topsoil was not caused by biological denitrification but by leaching from the padding. In previous studies, earthworm activity is a major N determinant in soil because earthworms mediate the conversion of organic N into inorganic N, forming a nitrogen-rich wormcast mainly in the form of organic N [16]. Therefore, this species of earthworm action zone (10 cm to 25 cm), wormcast, and nitrogen mineralization role contributed to the TN and NO_3-N variation at different depths. Moreover, the lower NO_3-N content in the underlying AS could also be ascribed to the rice straw as carbon source and the anoxic environment of this depth, which is conducive for denitrification.

To understand the removal mechanism for N, the nitrogen distribution of the *in situ* solution was analyzed. As shown in Fig. 3, the NH_3-N concentration of the *in situ* solution rapidly decreased in the upper 15 cm of the AS because of the colloid adsorption in the AS and wormcast [17]. However, the TN and NO_3-N concentrations increased with increasing depth. During the experimental process, inflow was distributed to the ecofilter, and the DO concentration was relatively high (mean value of 4.67 mg/L). Therefore, denitrification was weak in the top 30 cm of the

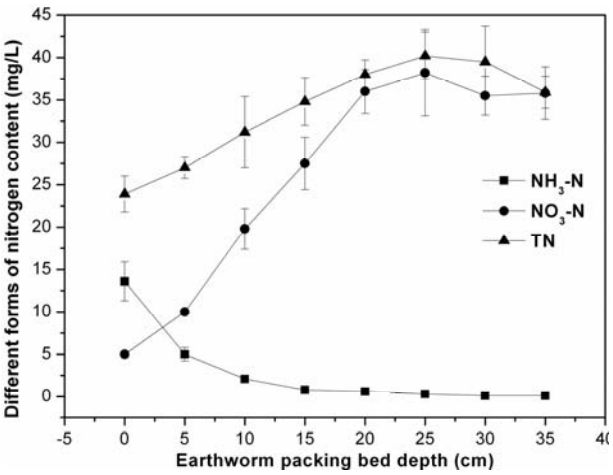

Fig. 3. Nitrogen distribution in *in situ* solution in an earthworm packing bed (artificial soil).

AS. Most of the soil had a negative charge, and only a certain amount of acidic soil containing a high quantity of Fe or Al oxides could accommodate a positive charge [18]. In the present study, the pH value of the soil was 7.04, and its chemical composition mainly consisted of silicon aluminium oxides [7]. Thus the soil particles were anions, similar to NO_3-N. A small amount of NO_3-N was adsorbed by the AS. Thus, the NO_3-N concentration increased in the 25 cm of padding because of the TN concentration. Consistent with TN and NO_3-N at the AS 25 cm to 35 cm depth, their concentrations decreased because of denitrification.

From the above results, a thickness of 15 cm to 20 cm was sufficient for the removal of NH_3-N content from the wastewater with approximately 56 mg/L of TN. However, from the view of TN removal, the thickness of the AS should be 35 cm to 40 cm to prevent the leaching of NO_3-N through the padding and provide good denitrification.

FTIR Analysis of the Artificial Soil, Sand, and Detritus

As indicated in Fig. 4, the absorbance peak intensities in the AS increased after wastewater treatment to 1,418.2,

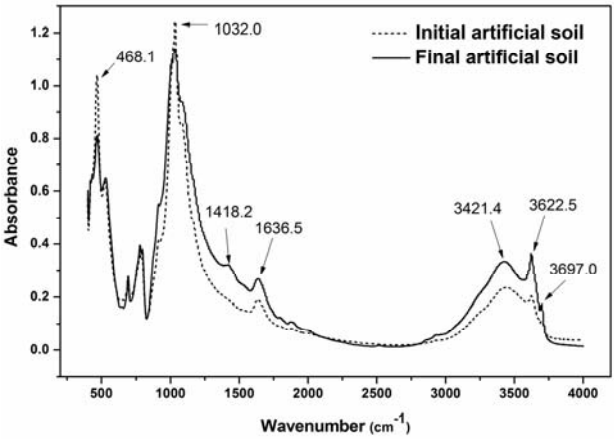

Fig. 4. FTIR spectra of the initial and final artificial soils.

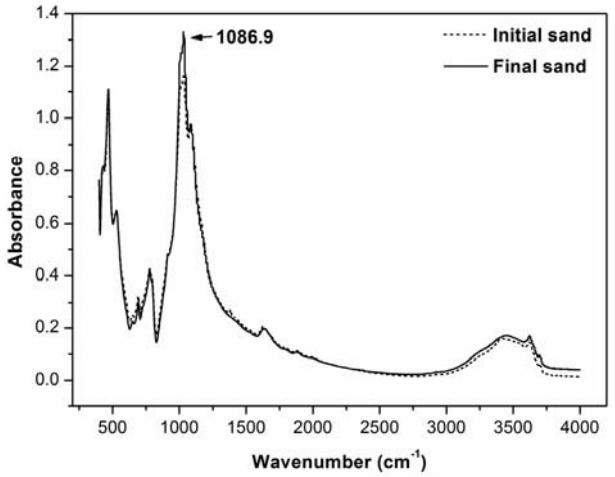

Fig. 5. FTIR spectra of the initial and final sand.

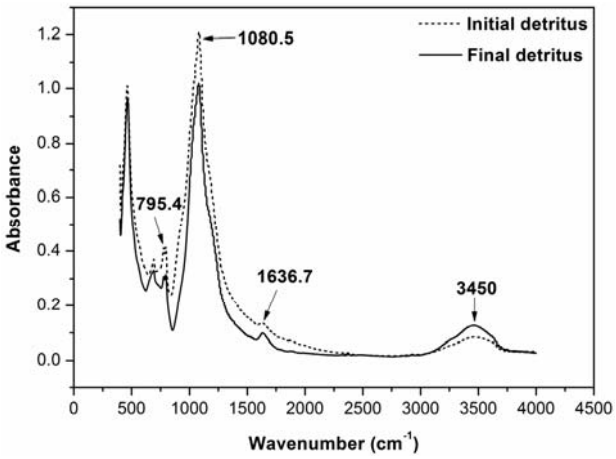

Fig. 6. FTIR spectra of the initial and final detritus.

1,636.5, 3,421.4, 3,622.5, and 3,697.0 cm^{-1}. These results were mainly caused by the roles of groups or bonds included in the soil molecules. In the region from 3,400 cm^{-1} to 3,750 cm^{-1}, absorbances are reported to correspond to hydroxyl (OH) stretching vibrations (polysaccharide), and amino peaks at 3,621 cm^{-1} [19]; the band position from 1,630 cm^{-1} to -1,650 cm^{-1} is assigned to the aromatic C=C, C=O in amide (I) [20]; the absorbance peak situated from 1,340 cm^{-1} to 1,490 cm^{-1} might be associated with the bending vibration of aliphatic, OH deformations, symmetric carboxyl (COO^-) stretch, and stretching of phenolic OH [19]. However, the intensity at bands of 1,032.0 cm^{-1} and 468.1 cm^{-1} slightly decreased after the wastewater treatment, and the absorbance of Si-O stretching vibrations was characteristic for the 1,032 cm^{-1} region. Those of Si-O bending vibrations are from 460 cm^{-1} to 475 cm^{-1} [21].

In Fig. 5, the increase in the relative intensity at the band in 1,086.9 cm^{-1} nearby assigned to the combination C-O stretching with O-H deformation of polysaccharides [22] occurred in the final sand. The plot of the FTIR spectra of detritus (Fig. 6) contained three obvious decreasing peaks situated in the 795.4, 1,080.5, and 1,636.7 cm^{-1} regions. The broad absorption band at 795.4 cm^{-1} was caused by the OH stretching vibration, and the 1,080.5 and 1,636.7 cm^{-1} assignments in the detritus could agree with those in 1,086.9 cm^{-1} in sand and 1636.5 cm^{-1} in AS, respectively. Furthermore, the increasing intensity of the absorbance peak at 3,450 cm^{-1} reflected the possible O-H stretching vibration of phenols present in detritus [19].

Most intensity variations of the absorbance peaks increased in AS, decreased in detritus, and changed slightly in sand compared with those in different media before and after wastewater treatment. This result indicated that AS OM was in a state of accumulation, whereas the detritus was in a state of decomposition. This phenomenon was presented by the increase in polysaccharides (3,400 cm^{-1} to 3,475 cm^{-1}), aromatic (C=C) component (1,630 cm to 1,650 cm^{-1}), and aliphatic moieties (1,340 cm^{-1} to 1,490 cm^{-1}) in AS, as well as the decrease in polysaccharides (1,080.5 cm^{-1}) and aromatic (C=C) component (1,630 cm^{-1} to 1650 cm^{-1}) in detritus. Furthermore, Fig. 5 shows that the OM content in sand was less decomposed or accumulated than that in the AS and detritus in VF. The spectral information of these results reflects a critical change in the OM quality of the media before and after sewage treatment, which has been consistently observed in river sediments [23]. However, the carboxylic signal (1,340 cm^{-1} to 1,490 cm^{-1} in AS and detritus) exhibited the spectral features of OM-rich padding enriched in carboxylic groups, which was contrary to a previous report on poor OM content following the increase in carboxylic content [24]. This effect may be related to the modification of the carboxylic group contents at AS by earthworm activities. Certain functional chemical attributes could evaluate the OM contents at the VF media. Thus, the functional group changes probably can explain why the AS served as the main filter, as well as why AS played an important role in transforming the C cycle in the earthworm packing bed.

Previous studies reported that amide N is the major form of nitrogen in soil OM and that the absorbance intensity of the amino groups is positively proportional to the TN contents in the peat, as revealed via FTIR [24, 25]. As shown in Figs. 4 and 6, the absorption peaks in AS (3,622.5 and 1,636.5 cm^{-1}) and detritus (1,636.7 cm^{-1}) were assigned to the amino or amino-group, whereas the intensity of the variations at different media had no positive correlation with TN, NH_3-N, and NO_3-N contents (Fig. 2). Unlike soil in a natural environment, the N distribution in VF is complicated because it is not only affected by adsorption, volatilization, assimilation, nitrification, and denitrification functions, but also by continuous wastewater addition and earthworm reinforcement roles. Therefore, TN changes in the VF media cannot be indirectly reflected via FTIR analysis.

Conclusion

This study showed how the OM, NH_3-N, NO_3-N, and TN contents changed in AS at different earthworm packing bed depths. The preferable earthworm packing bed thickness was 35 cm to 40 cm, which was proven conducive for both NH_3-N and TN removal. The FTIR spectra in different

matrices suggested that the adsorption intensities of certain functional groups were different before and after synthetic wastewater treatment, and AS played a major role in transforming C cycles in VF. Moreover, the aliphatic and aromatic groups might be related with the OM quantity in VF media, but not with N contents.

Acknowledgements

The authors thank the National Water Pollution Project for Taihu Lake Pollution Control of China (2012ZX07101-007) for its financial support.

References

1. SHAO Y. Y., PEI H. Y., HU W. R. Nitrogen removal by bioaugmentation in constructed wetlands for rural domestic wastewater in autumn. Desalin. Water. Treat. **51**, 6624, **2013**.
2. WU Y. F., ZHU W. B., LU X. W. Identifying key parameters in a novel multistep bio-ecological wastewater treatment process for rural areas. Ecol. Eng. **61**, 166, **2013**.
3. SOMBATSOMPOP K., SONGPIM A., REABROI S., INKONG-NGAM P. A comparative study of sequencing batch reactor and movingbed sequencing batch reactor for piggery wastewater treatment. Maejo. Int. J. Sci. Tech. **5**, 191, **2011**.
4. KUMAR T., RAJPAL A., BHARGAVA R., PRASAD K. S. H. Performance evaluation of vermifilter at different hydraulic loading rate using river bed material. Ecol. Eng. **62**, 77, **2014**.
5. LIU J., LU Z. B., ZHANG J., XING M. Y., YANG J. Phylogenetic characterization of microbial communities in a full-scale vermifilter treating rural domestic sewage. Ecol. Eng. **61**, 100, **2013**.
6. MORAND P., ROBIN P., POURCHER A. M., OUDART D., FIEVET S., LUTH D., CLUZEAU D., PICOT B., LANDRAIN B. Design of an integrated piggery system with recycled water, biomass production and water purification by vermiculture, macrophyte ponds and constructed wetlands. Water. Sci. Technol. **63**, 1314, **2011**.
7. FANG C. X., ZHENG Z., LUO X. Z., GUO F. H. Effect of hydraulic load on domestic wastewater treatment and removal mechanism of phosphorus in earthworm ecofilter. Fresen. Environ. Bull. **19**, 1099, **2010**.
8. WANG L. M., ZHENG Z., LUO X. Z., ZHANG J. B. Performance and mechanisms of a microbial-earthworm ecofilter for removing organic matter and nitrogen from synthetic domestic wastewater. J. Hazard. Mater. **195**, 245, **2011**.
9. SHAO L., XU Z. X., JIN W., YIN H. L., ZHU B. R. Nitrate removal from wastewater using rice strawas carbon source and biofilm carrier. Environ. Sci (China). 30, 1414, 2009.
10. State Environmental Protection Administration. Water and wastewater monitoring and analysis methods. 4th.; Beijing, China, pp. 210-281, **2002**.
11. LIU G. S. Soil Physical and Chemical Analysis & Description of Soil Profiles, 1st ed.; Beijing, China, pp. 5-37, **1996**.
12. MEKONEN K., TESFAHUNEGNG B. Impact assessment of soil and water conservation measures at Medego watershed in Tigray, northern Ethiopia. Maejo. Int. J. Sci. Tech. **5**, 312, **2011**.
13. BEMARDI A. C. C., MOTA E. P., CARDOSA R. D., MONTE M. B. M., OLIVEIRA P. P. A. Ammonia volatilization from soil, dry-matter yield, and nitrogen levels of Italian ryegrass. Commun. Soil. Sci. Plan. **45**, 153, **2014**.
14. ZHAO Y. J., HUI Z., CHAO X., NIE E., LI J. H., HE J. ZHENG Z. Efficiency of two-stage combinations of subsurface vertical down-flow and up-flow constructed wetland systems for treating variation in influent C/N ratios of domestic wastewater. Ecol. Eng. **37**, 1546, **2011**.
15. BHATNAGAR A., SILLANPÄÄ M. A review of emerging adsorbents for nitrate removal from water. Chem. Eng. J. **168**, 493, **2011**.
16. AMOSSE J., BETTAREL Y., BOUVIER C., BOUVIER T., DUC T. T., THU T. D., JOUQUET P. The flows of nitrogen, bacteria and viruses from the soil to water compartments are influenced by earthworm activity and organic fertilization (compost vs. vermicompost) . Soil. Biol. Biochem. **66**, 197, **2013**.
17. ROCHETTE P., ANGERS D. A., CHANTIGNY M. H., GASSER M. O., MACDONALD J. D., PELSTER D. E., BERTRAND N. NH_3 volatilization, soil NH_4^+ concentration and soil pH following subsurface banding of urea at increasing rates. Can. J. Soil. Sci. **93**, 261, **2013**.
18. KETROT D., SUDDHIPRAKAM A., KHEORUENROMNE I., SINGH B. Interactive effects of iron oxides and organic matter on chargeproperties of red soils in Thailand. Soil. Res. **51**, 222, **2013**.
19. SIMKOVIC I., DLAPA P., DOERR S. H., MATAIX-SOLERA J., SASINKOVA V. Thermal destruction of soil water repellency and associated changes to soil organic matters as observed by FTIR spectroscopy. Catena. **74**, 205, **2008**.
20. HAFIDI M., AMIR S., REVEL J. C. Structure characterization of olive mill waster-water after aerobic digestion using elemental analysis, FTIR and 13C NMR. Process. Biochem. **40**, 2615, **2005**.
21. NAYAK P. S., SINGH B. K. Instrumental characterization of clay by XRF, XRD and FTIR. B. Mater. Sci. **30**, 235, **2007**.
22. GRUDE M., LIN J. G., LEE P. H., KOKOREVICHA S. Evaluation of sewage sludge-based compost by FTIR spectroscopy. Geoderma. **130**, 324, **2006**.
23. GALLÉ T., LAGEN B. V., KURTENBACH A., BIERL R. An FTIR-DRIFT study on river sediment particle structure: implications for biofilm dynamics and pollutant binding. Environ. Sci. Technol. **38**, 4496, **2004**.
24. CHAPMAN S. J., CAMPHBELL C. D., FRASER A. R., PURI G. FTIR spectroscopy of peat in and bordering Scots pine woodland: relationship with chemical and biological properties. Soil. Biol. Biochem. **33**, 1193, **2001**.
25. CLINTON P. W., NEWMAN R. H., ALLEN R. B. Immobilization of ^{15}N in forest litter studied by 15N CPMAS NMR spectroscopy. Eur. J. Soil. Sci. **46**, 551, **1995**.